Renewable and Sustainable Energy Reviews 33 (2014) 60–73

Contents lists available at ScienceDirect

Renewable and Sustainable Energy Reviews

journal homepage: www.elsevier.com/locate/rser

Performances and numerical optimization of a novel thermal solar collector for residential building

Gilles Notton*, Fabrice Motte, Christian Cristofari, Jean-Louis Canaletti

University of Corsica, UMR CNRS 6134, Research Centre of Vignola, Route des Sanguinaires, F-20000 Ajaccio, France

A R T I C L E I N F O

Article history:
Received 25 July 2013
Received in revised form
14 January 2014
Accepted 31 January 2014
Available online 20 February 2014

Keywords:
Thermal solar collector
Building-integration
Modelling
Experimentation
Optimization

A B S T R A C T

A new flat-plate solar collector with high building integration was designed and a prototype of this collector was built. The implemented experimentations showed that the performances of this solar collector can be improved. A numerical thermal model using a finite difference and developed in Matlab® environment was validated. Then, a modelling of the complete solar domestic hot water system (solar collector + water storage + piping) was implemented. The performances of this system were calculated for various solar collector configurations as number and position of water pipes, air layer thickness, thermal insulation thickness… Three solar fractions are defined and used in the optimization procedure. An optimized solar collector structure is finally presented.

Contents

* Corresponding author. Tel.: +33 495524152; fax: +33 495524142.
E-mail addresses: gilles.notton@univ-corse.fr (G. Notton), motte@univ-corse.fr (F. Motte), cristofari@univ-corse.fr (C. Cristofari), canaletti@univ-corse.fr (J.-L. Canaletti).

http://dx.doi.org/10.1016/j.rser.2014.01.061
1364-0321

1. Introduction

A European citizen uses 36 l of 60 °C hot water daily with tendency for increase in future [1]. The required energy to produce hot water is rising slightly because the comfort level sought now is greater than in the past. In older buildings, this sector represents only 6% of overall energy consumption, but with a reduced heating need mainly due to a better thermal insulation, the hot water production can reach 30% of energy consumption in a new housing. A solar collector is a good and sustainable solution for heating water and can efficiently provide up to 80% of the hot water needs, without fuel cost or pollution and with a minimal O&M expense. The following observations explain the researches renewal in view to improve and conceive new thermal collectors:

- the increase of the water heating part in the housing consumption;
- the development of new sustainable solutions for reducing the building consumption; and
- the strong growth of the solar thermal market.

Builders recognize more and more that building high energy efficient housings is a sensible, ethical, ecological idea and workable at medium and long-term.

A large web survey concerning architectural integration of solar technologies (addressed to about 170 European architects and other building professionals) presented by Munari Probst and Roecker [2] showed that the architectural integration is a major issue in the development and spreading of solar thermal technologies. For the past several years, the solar installations are becoming an architecture element; we note a need for the integration, for reducing the visual impact of solar systems which can even be removed from the roofs. D'Antoni and Saro [3] reviewed the literature on high-capacitance solar thermal collectors, showing the various variants and applications, and presenting separated solar collectors, partially or fully building integrated.

The common developed methods in order to reduce the negative architectural impact are to decrease the size of the solar collectors in using hybrid PV/Th solar collectors producing simultaneously electricity and heat or to develop more efficient solar systems, i.e. to increase the production per meter square. Another interesting approach is to give a double function to some energetically passive parts of the house.

1.1. PV/TH hybrid solar collector

The first PV/Th solar collector appeared in the 1970s [4]; the production of energy (heat and electricity) is increased for a same collector area reducing the cost and the amount of required space [5]. Several reviews on the PV/Th development were realized by Chow [6], Ibrahim et al. [7] and Tyagi et al. [8] for air and liquid types, by Kumar and Rosen [9] and Hussain et al. [10] for air only PV/Th collectors. Vats and Tiwari [11] compared several PV technologies. PV/Th collectors sometimes provide energy to a solar still [12] which is, then, electrically autonomous; they also may be coupled to a heat pump [13]. A building façade can be transformed directly into a PV/Th converter: the air is heated and circulates between the PV modules and the wall [14].

1.2. More efficient thermal solar collector

Regarding the more efficient solar collectors, there are concentrated solar collectors (for low or medium temperature (high temperature cannot be used in buildings), vacuum solar collectors, solar collectors using new nanofluids, or a combination of these solutions.

Vacuum solar collectors, with the combination of a selective absorber and the deletion of the natural convection between glass and absorber give good results, particularly for high fluid temperatures or low ambient temperatures [15]. These collectors are more fragile and more costly than conventional ones. Robin [16], using vacuum tubes ICR (Internal Cylindrical Reflector) manufactured by Schott Solar, developed a patented solar thermal glazing with a high building integration. Chen et al. [17] developed and tested a vacuum solar collector made in acrylic. Rassamakin et al. [18] manufactured aluminium profiled heat pipes for thermal solar collectors able to be integrated into building façades and roofs. Glembin et al. [19] investigated the impact of low flow rates on the efficiency of coaxial vacuum tube collectors.

Concentrated solar collectors, for low and medium temperature can be used in buildings. A concentrating solar thermal collector, using plastic material in substitution of metallic ones was developed for economical supply of heat between 40 and 90 °C [20]. Kalogirou [21] presented a review about low concentration solar collectors. Nkwetta et al. [22] compared concentrated and non-concentrated solar vacuum collectors. The utilization of concentrated evacuated tube solar collectors are more and more used for heating and cooling with higher outlet temperature and lower heat losses [23–25].

Nanofluids are found to have both good stability and useful optical and thermal properties as solar absorbers in solar collectors [26]. Therefore, numerous studies are developed. A detailed study of the particular boundary layer flow, due to the non-linear stretching of a flat surface in a nanofluid, taking into account the influence of numerous parameters was realized by Rana and Bhargava [27]. Rana and Bhargava [28] investigated also the steady, two dimensional, mixed convection laminar boundary layer flow of incompressible nanofluid along a permeable vertical semi-infinite flat plate with a magnetic field; this breakthrough study may be important for the next-generation of solar film collectors and heat exchangers technology. A complete and interesting review on the utilization of such nanofluids for solar applications was made by Javadi et al. [29]. Tyagi et al. [30] investigated theoretically the utilization of a nanofluid composed of water and aluminium nanoparticles as an absorbing medium; they showed that the presence of nanoparticles increases the absorption by 9 compared with pure water and improves the efficiency of the solar collector by 10%. Yousefi et al. [31] studied experimentally the influence of a MWCNT nanofluid on the efficiency of a flat plate solar collector and showed that according to the mass fraction and the presence of surfactant, the efficiency can increase substantially. Diathermic oils, based on nanofluid can have interesting properties for solar application and their thermal conductivities was experimentally determined [32]; a problem of sedimentation occurs with the utilization of nanofluids in a conventional solar collector: this problem was studied experimentally by Colangelo et al. [33] and they showed that it depends on the fluid velocity and the volume fraction of the solid phase, the water–Al_2O_3 fluid improves the solar collector performances and avoids the sedimentation. Using a nanofluid in replacement of water improves the performances and consequently reduces the surface occupied by the solar collector, for a same productivity by about 37% [34].

1.3. Double function of passive part of building

Numerous architectural projects with solar system integration were realized all around the World and it is impossible to list all of



Fig. 1. The patented solar collector H2OSS®.

them, but we present here some original concepts of new solar collectors with a high building integration. Hassan and Belliveau [35] designed a horizontal roof solar collector replacing the ridge of the roof. De Beijer [36] developed a solar collector with one tube assembled into the other, the inner tube is used as a storage tank and the outer one is the absorber, the space between them is vacuum-filled. When the outer tube is heated, the water placed in this space evaporates and condenses on the colder side of the inner tube. This collector is used as ridge tiles of a roof due to its cylindrical form. Huang et al. [37] developed a solar collector as parapet or sun-shading canopy of a building; it is used as a construction material and reduces greatly the overall cost.

These solutions are very promising and can be coupled together for reaching high performances with a low increase of the cost. The concept developed in this paper belongs to this third category.

Applying our “basic” idea i.e. giving an active function to passive parts of building and by a similar approach to that used few years ago, for a solar air collector integrated into a shutter [38], we developed a novel patented concept [39] of water solar collector, using well-known technologies, inserted into a gutter.

In this paper, we present in the first paragraph the new concept of water solar collector called H2OSS and the experiment implemented in view to test its thermal performances and to validate the numerical thermal model. Then, we will show the main experimental results concerning the thermal performances and the main negative points due to its particular shape. In the second part, the numerical model developed in view to simulate the thermal behaviour of the total thermal loop with the solar collector, the piping, the storage tank, … is shown. This model consists of two sub-models, the first one for the solar collector itself presented in detail and validated in [40] and the second one for the storage and the thermal loop inspired by the work of Haillot et al. [41]. This numerical model being in place, we will use it for determining the best configuration of thermal system: we will address individually the influence of various parameters as flow rate, air layer and insulation thickness, glass emissivity, etc. … and for each parameter the optimal value will be determined. Therefore, we will present a new improved configuration of the solar collector which will serve as a basis for the development of a new prototype.

2. Presentation of the solar collector and of the thermal experiment

2.1. The water solar thermal collector

The patented solar water collector H2OSS® presents a high building integration and cannot be seen from the ground because it is inserted within a drainpipe (Fig. 1); this gutter conserves its rainwater evacuation role. It can be used both on east, west or south oriented walls (the collector being oriented south into the drainpipe). A north orientation is excluded due to important shading effects. The canalizations connecting the house to the solar collector are hidden in the vertical drainpipe. An installation consists in several connected modules. One module is about 1 m long by 0.1 m wide (individual houses), larger modules can be developed for buildings. The number of modules depends on the drainpipe length.

The structure of the H2OSS® solar collector is composed by a glass (green house effect), an air layer, a highly selective absorber and a thermal insulation layer (Fig. 2). The cold fluid flows from the tank through the inferior insulated tube and then in the upper tube in thermal contact with the absorber.

2.2. The experimentation

The experimentation (Fig. 3) has for objectives to test the thermal behaviour, to validate the thermal model and to improve the performances by some parameters adjustments. It is located on the laboratory site situated in the gulf of Ajaccio (latitude: 41°55′N; longitude: 8°55′E) at about 200 m from the Mediterranean Sea and at an altitude of 70 m. This experimentation allows to operate closer to the European Standard EN 12975-1 [42]: 4 rows of 4 thermal modules (1.8 m²), connected in serial or parallel, are fixed on a solar tracker for a better control of the solar intensity and direction.

The solar modules are connected to a thermal loop which regulates the input fluid temperature in heating the fluid if it is too cold and cooling it in the other case using an air cooler. Every minute are collected: solar irradiance on the collector plane (measured by a Kipp & Zonen CM11 pyranometer), ambient temperature, humidity, wind speed and direction, fluid flow rate and input and output fluid temperatures (for each module).

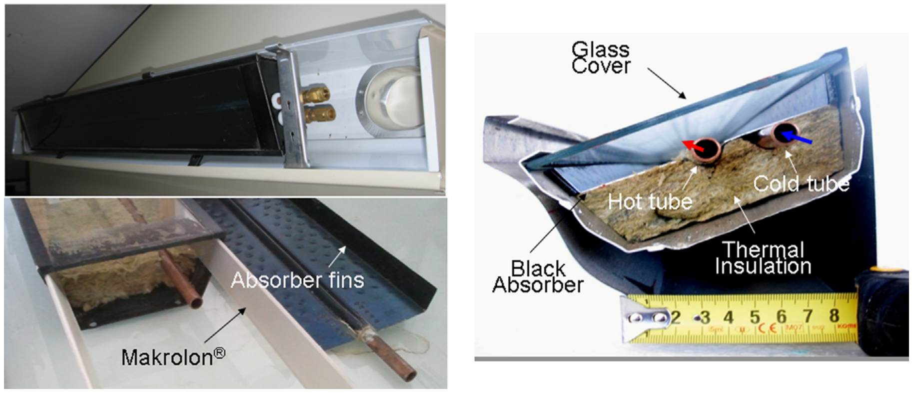
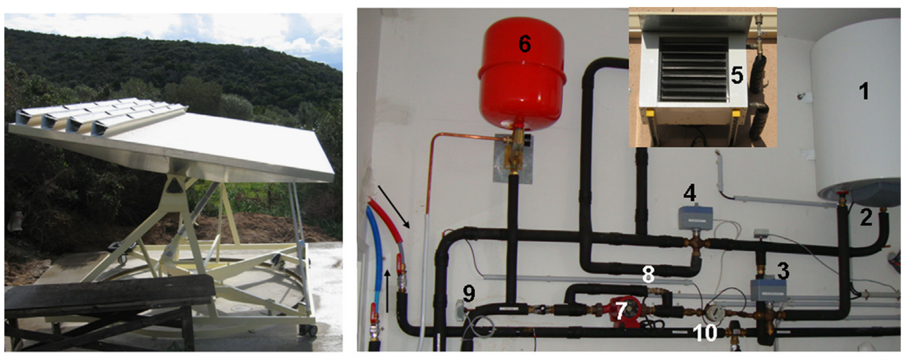


Fig. 2. The thermal solar module structure.



1. Water heater with electrical resistance 2.Temperature sensor (dry cooler gate control). 3. Water heater gate. 4. Dry cooler gate 5. Dry cooler (outdoor). 6. Expansion tank. 7. Pump. 8. Flow rate adjustment. 9. Temperature sensor (water heater gate control. 10. Flow meter

Fig. 3. The experiments: the solar tracker with H2OSS modules and the thermal loop.

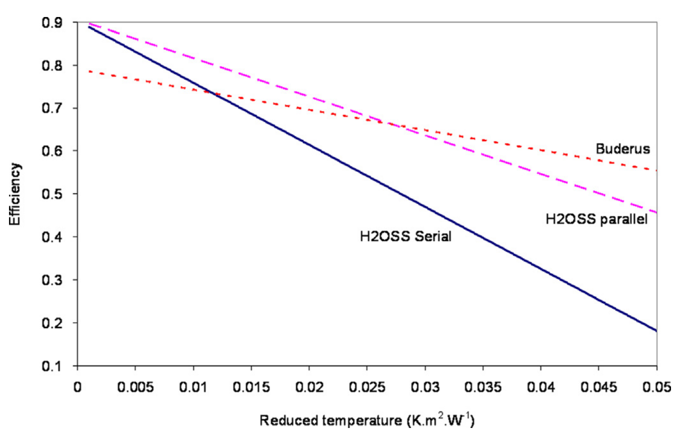


Fig. 4. Efficiencies versus the reduced temperature for H2OSS and Buderus SKN. 3.0.

This experiment allows to calculate the performances of the new solar collector and to compare them with the performances of a conventional solar one (Buderus 3.0) measured on the same site for a same collector surface area. Fig. 4 shows the efficiency (η) in stationary conditions versus the reduced temperature Tr [43] for the Buderus solar collector and.the H2OSS in parallel and serial configurations. The efficiencies were calculated experimentally for various measured reduced temperature and then, a linear regression is applied in view to determine the optical efficiency and the thermal losses according to Eq. (1):

$$\eta = -KTr + B \text{ with } Tr = (T_m - T_{amb})/\Phi \quad (1)$$

Table 1
Optical efficiency and thermal losses.

	Buderus SKN 3.0.	H2OSS serial	H2OSS parallel
Optical efficiency B	0.786	0.890	0.906
Thermal losses, *K*	4.33 W m^{-2} K^{-1}	13.50 W m^{-2} K^{-1}	8.99 W m^{-2} K^{-1}

with Φ the solar irradiance, T_m the average temperature, T_{amb} the ambient temperature, B the optical efficiency (dimensionless) and K the thermal losses (W m^{-2} K^{-1}) [44].

The values of the optical efficiency and of the thermal losses are given in Table 1.

If the optical efficiency is high, the coefficient relative to the thermal losses reveals weak performances. This difference is due to the geometry of the H2OSS® modules. The thermal losses by the sides of the modules are more important and so the performances decrease rapidly when the reduced temperature increases. Consequently, the performances of the H2OSS collector are better with a low reduced temperature i.e. it works better when the temperature of the input water is low; then, it is more interesting to use a water storage tank with a thermal stratification and therefore to work at low flow rate; in these conditions, the water coming from the tank to the solar collector will be colder.

We show in Fig. 5. the thermal performances for the two solar collectors for two days with similar meteorological conditions. The input water temperature is 60 °C, a high reduced temperature unfavourable to the H2OSS collector. The meteorological data, the water temperatures and the useful thermal power per m² are plotted in Fig. 4.

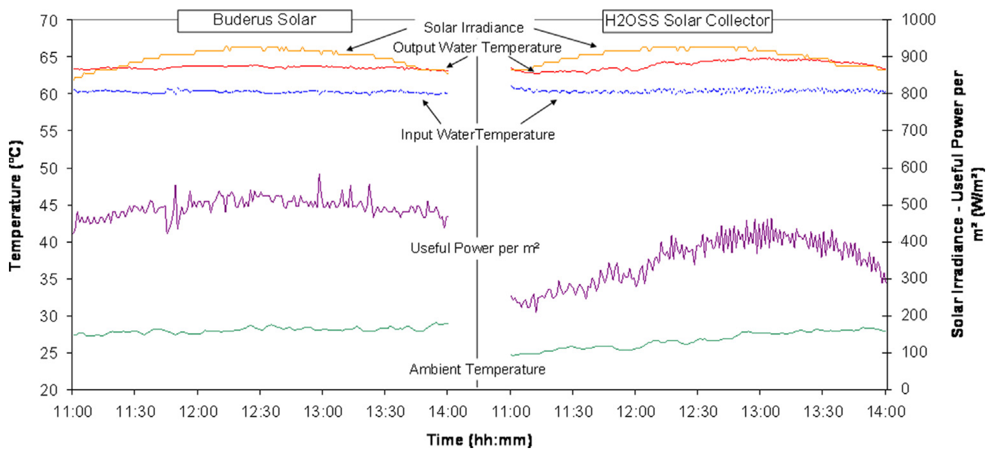


Fig. 5. Comparison of the two solar collectors performances.

We note that, around the solar zenith, the gap between the two useful powers is about 100 W m^{-2}. This period is unfavourable to the H2OSS collector because the reduced temperature is high. In decreasing this temperature, the gap will be reduced and reversed when the reduced temperature will reach about 0.013 K m²/W as seen in Fig. 4.

Consequently, the thermal performances of the H2OSS collector are good for low reduced temperatures but the thermal losses are greater than for a conventional solar collector with simple cover and selective absorber.

It would have been useful to compare the thermal performances with other solar collector models but the previous results were obtained for outdoor meteorological conditions and a good comparison can be realized only under same conditions; it is difficult to have several solar collectors models on the same site. Moreover, the objective of this work was to improve the H2OSS collector and the experiment was realized in view to observe the main problems encountered with the particular shape of this solar collector.

Thanks to the use of a numerical simulation, it is possible to test various new configurations of the solar system using the H2OSS collector and to improve its efficiency by some well chosen modifications.

3. The thermal model

A brief description of the model used for the solar domestic hot water system is presented in Fig. 6 and detailed in two previous papers [40,41]; it consists of two main models:

- A thermal model of the H2OSS module which calculates various temperatures into the solar collector [40].
- A thermal model of the hydraulic loop with the water storage and the water distribution circuit developed by Haillot et al. [41].

3.1. The H2OSS solar collector

The particular geometry of the H2OSS solar collector with its lateral faces much wider than in a conventional collector relatively to its collecting surface, generates a specific thermal behaviour.

We developed a bi-dimensional model with thermal transfers composed of a serial assembling of one-dimensional elementary models. The domain is broken up into elementary isotherm volumes, and for each node (97 nodes), we write a thermal balance

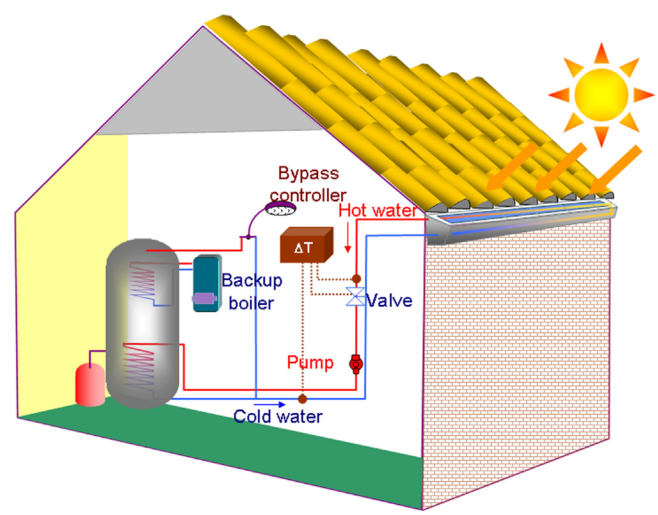


Fig. 6. The solar domestic hot water system.

equation using an electrical analogy. All parameters of this model can be easily changed as module length, number of modules, physical properties of materials, geometry, convective coefficients, contact resistances, … in such a way that the influence of future changes on the thermal performances of solar module can be estimated.

The solar collectors can be connected in serial or parallel; in the first case, in the flow direction, the output fluid temperature of the first module becomes the input fluid temperature of the next one (see Fig. 7); in the second case, the output temperature is the same for all the lines of modules and the total water flow rate is the sum of the flow rates of each line.

We obtain a system of 97 differential equations solved using an iterative method (each differential equation is solved using the implicit Euler method). The input variables for this model are: the solar irradiance Φ, the ambient temperature T_{amb}, the air speed v, the sky temperature T_{sky}, the cold fluid temperature for the first module and the gutter temperature T_{gutter}.

This thermal model has been implemented and validated from experimental data. A solar module was specially instrumented with 9 thermal sensors measuring the surface temperature in 9 specific points spread over the glass, the blade, the absorber, the insulation and the two faces [40]. The water output and input temperatures were also recorded.

The experimental validation showed that the model had a good accuracy with the measured data: the relative root mean square

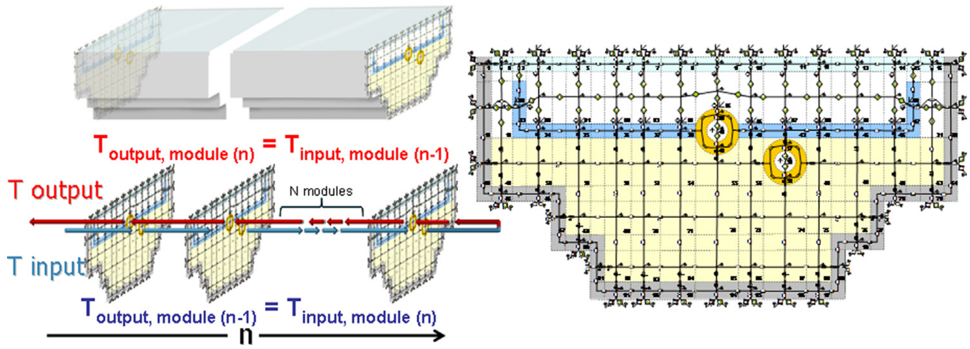


Fig. 7. Electrical analogy of the solar thermal collector and serial connexion.

errors are around 5% for the water temperatures and between 4.6% and 10% for the internal ones [40].

3.2. The hydraulic loop

During the experimental phase, we noted that one of the essential problems was the hydraulic resistance due to linear structure of the H2OSS collector. Consequently, it would be wise that this solar system works in low flow rate conditions. As well as reducing the hydraulic losses, the low rate regime has also other advantages as [45]:

- Thermal stratification: In low flow conditions, the outlet temperature from the solar collector is higher than in conventional conditions; thus, a high degree of thermal stratification occurs inside the heat storage; moreover, the temperature at the top of the storage is closer to the desired load temperature. Therefore, the auxiliary energy consumption will be decreased when the solar fraction increases. With highly stratified heat storage, the temperature of the water returning to the solar collector will be lowered and the working periods of the solar collector will be longer; in this way, the energy produced by the solar collector increases [46,47].
- Piping in the solar collector loop: the low flow conditions allow to use smaller pipes, in this way less material is used for pipes and insulation and the heat losses are reduced.
- Pump: The energy consumption of the circulation pump is decreased; it is very important in our case because with a high flow, the hydraulic losses are high and the energy for the fluid circulation is important.

The thermal loop behaviour is simulated using a numerical code based on a nodal approach [41,48]. It is divided in 19 nodes: 7 for the fluid circulation, 10 for the storage tank (optimal number of nodes in view to take into account optimally the thermal stratification [45] and 2 for the water inlet and outlet in the storage (see Fig. 8). The water temperature at the outlet of the solar collector and the average temperature of the solar absorber are obtained from the model of the solar collector, keeping in mind that 97 temperatures in the solar collector must be computed for determining these two temperatures.

The energy balance, in 1-D, is applied and an iterative method is used to solve the first order differential equations. A "reversion-elimination mixing algorithm" based on a thermal mix of some storage tank nodes allows to obtain a correction factor in order to have a positive temperature gradient from the bottom to the top of the tank [49,50]. This factor is used to simulate the thermal stratification in the tank.

The tubes between the tank and the solar collector are 20 m long for half inside (the ambient temperature is then the temperature into the building) and for half outside of the building; the thermal losses are taken into account.

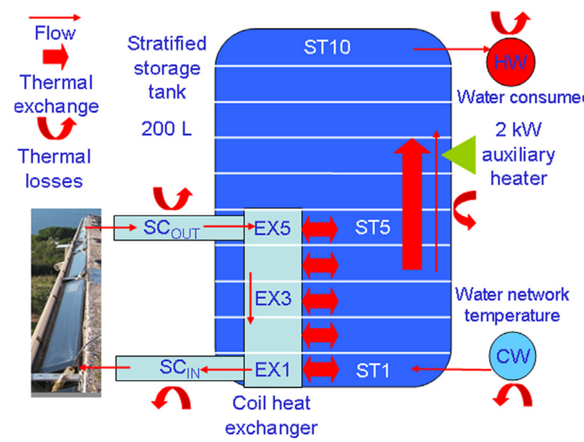


Fig. 8. Model nodes definitions [9].

The coil heat exchanger is modelled by 5 nodes and the thermal power between the heating fluid and the water into the tank is calculated using the ε-NTU method [51]. The domestic hot water is extracted according to a given daily water consumption profile [52] (Fig. 9) from the top of the tank (Node ST10), then used at temperature T_{HW}; in the same time an equivalent amount of fresh water at temperature T_{CW} (depending on the month and the site) is introduced into the tank in the node ST1. The thermal losses between the water distribution network and the tank and between the storage tank and the water network of the building are taken into account.

The French Scientific and Technical Centre of Building (CSTB) analysed the performances of 120 solar thermal systems working in real conditions and prescribes to give to the user a water at 50 °C [53]. This temperature allows to reduce the energy consumption but the risk of legionella development exists, thus for avoiding it, it is necessary to use a thermal flash at 70 °C [53,54]. The auxiliary heating is activated when the temperature in the node ST8 falls under 50 °C and stopped when it reaches 55 °C.

Generally, in a conventional solar system, the pump is switch on or off in comparing the temperature in the bottom of the tank with the output temperature of the solar collector; but, the collector is inclined and the hot fluid climbs by natural convection to the temperature sensor situated on the top of the collector when the pump is stopped; for the H2OSS collector, the input and the output of the thermal fluid is at the same level what annihilates the natural fluid movement and does not allow to measure the increase of the temperature. Thus, another mode of regulation is chosen: the pump is activated when the difference between the absorber and the ST1 node exceeds the following threshold dON defined by:

$$dON = 0.16(T_{ST1} - 20) + 9 \tag{2}$$

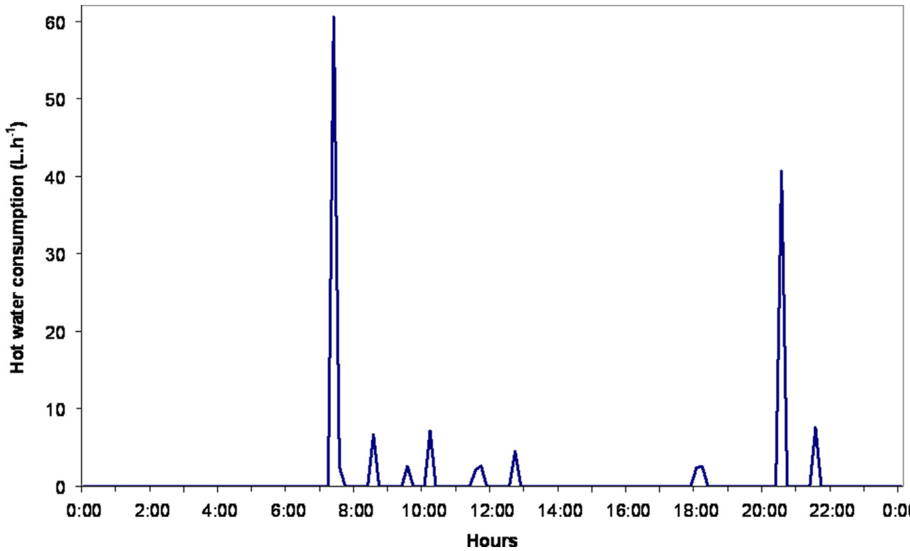


Fig. 9. End-user daily load profile [52].

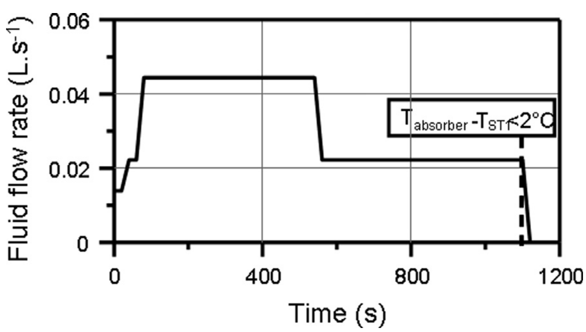


Fig. 10. Flow rate variation of the pump.

The pump is switch-on when:

$$9 < dON < 17 \text{ and } T_{absorber} - T_{ST1} > dON \quad (3)$$

Then the flow rate is regulated as seen in Fig. 10: after a rapid increase of the flow rate, the pump runs at peak power and then continues at half capacity and it is stopped when ($T_{absorber} - T_{ST1}$) is less than 2 °C.

This regulation method is used by some thermal solar collector manufacturer as Wagner & Co. [55] and Buderus [56].

The model described for the thermal loop was tested and validated by Haillot et al. [41] from data measured in 2008. The comparison between experimental and computed data conduced to a relative root mean square error of 8.6% for the yearly average solar fraction; these results validate this thermal loop model. In view to illustrate the thermal behaviour of the storage, we plotted in Fig. 11 the evolution of the temperatures ST1 to ST10 into the tank and we see clearly the stratification phenomenon that occurs.

The two models have a good accuracy and can be coupled to simulate the thermal behaviour of the total solar system. The solar collector model calculates 97 temperatures but only the output water temperature and the absorber temperature are introduced in the thermal loop model.

4. Optimisation of the solar collector structure

Our objective is to improve the performances of the solar collector H2OSS in optimizing some parameters as the air layer thickness, the emissivity of the cover, the thermal insulation thickness, the pipes positioning but also of the working conditions as the fluid flow rate. This optimization is realized through several simulations using the two coupled models described previously in varying the configuration of the system.

4.1. The optimisation procedure

In view to choose the optimal configuration, we calculate during each simulation the following data:

- the working time of the pump and its electrical energy consumed;
- the working time of the electrical auxiliary heater and its electrical energy consumed;
- the thermal energy drawn to the storage tank i.e. useful for the user;
- the thermal energy produced by the solar system (solar and electrical);
- the part of the thermal energy produced by the solar resource; and
- the thermal losses by the storage tank and the distribution water network.

From these data, we defined three solar fractions:

- SF: the conventional Solar Fraction which is the ratio of the total solar energy delivered to the tank $E_{Thermal,Solar}$ (kWh) and the total energy delivered to the tank $E_{Thermal}$ (kWh). $E_{Thermal}$ is the sum of the solar energy delivered to the tank and the auxiliary energy delivered to the tank $E_{Electrical,AuxHeat}$.

$$SF = E_{Thermal,solar}/E_{Thermal} = E_{Thermal,solar}/(E_{Thermal,solar} + E_{Electrical,AuxHeat}) \quad (4)$$

- SF^{+}: we noted during the experiment that important hydraulic losses occur in the solar collector due to the serial connexion of the thermal modules. These hydraulic losses require the use of an electrical pump with a high peak power and then a high electrical consumption for the fluid circulation. This supplementary electrical energy due to the pump working is taken into account in the calculation of the solar fraction and we add the electrical energy consumed by the pump $E_{Electrical,pump}$ to the

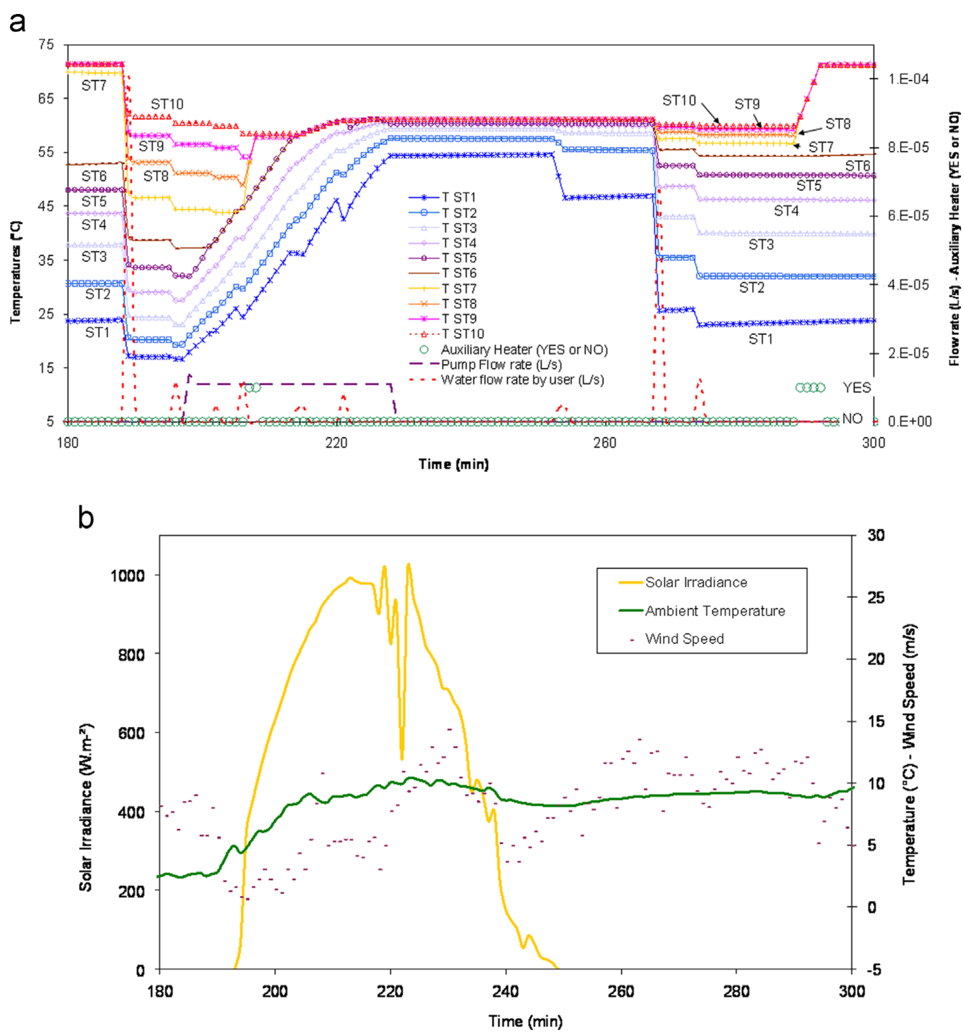


Fig. 11. (a) Illustration of the thermal stratification into the storage tank. (b) Meteorological conditions.

electrical energy used for the auxiliary heating:

$$SF^{+} = E_{Thermal,solar}/(E_{Thermal,solar} + E_{Electrical,AuxHeat} + E_{Electrical,pump}) \quad (5)$$

- SF^{++}: the value of electrical energy and thermal energy differs by the form of energy. Electricity is a high-grade form of energy since it is converted generally from thermal energy. To take into account this consideration, Huang et al. [57] suggest using an energy-saving efficiency called also overall thermal efficiency [58–60]; in this efficiency the thermal energy is converted into electrical energy via a electric power generation efficiency $\eta_{Ther-Elec}$ considering a conventional power plant. $\eta_{Ther-Elec}$ is taken equal at 0.38 [57–60]. This formulation suggests energy equivalence between electricity and thermal energy with an electrical-to-thermal ratio equal to 2.63 (1/0.38). To take into account this difference of quality of energy, we introduced the solar fraction SF^{++} converting the electrical energy in thermal one

$$SF^{++} = E_{Thermal,solar}/[E_{Thermal,solar} + (E_{Electrical,AuxHeat} + E_{Electrical,pump})/\eta_{Ther-Elec}] \quad (6)$$

We saw during the experiment (see Section 1.2) that the main problem is the heat loss due to the particular shape of the H2OSS collector. The objective being to reduce the temperature of the absorber, we wanted to test, after preliminary studies, a new configuration of the H2OSS collector called New Version (Fig. 12).

Our optimisation is realized on the basis of the three solar fractions and for a solar thermal system used by a family of 4 persons living in Corsica and composed by 35 serial connected modules H2OSS (4 m²) and a storage tank of 200 L.

First, we verified that the utilization of 35 serial solar modules does not conduce to a saturation of the temperature i.e. that the water temperature continues to increase. Fig. 13 shows, in steady-state, the evolution of the water temperature versus the number of solar thermal modules (for a solar irradiance = 750 W m^{-2}, an ambient temperature = 25 °C, a wind speed = 1 m s^{-1} and a flow rate = 60 L h^{-1}) for the two versions of the solar collector.

We clearly note a more rapid phenomenon of saturation for the new version of solar collector but we can conclude that it is possible to install efficiently in serial 50 solar thermal modules i.e. 50 m of gutter (rarely available in a conventional house).

We used a pump for the fluid circulation with an electrical power calculated proportionally to the flow rate between 30 W for 15 L h^{-1} and 250 W for 200 L h^{-1}.

Our calculations are realized for a winter month (January) and a summer one (July) from meteorological data collected on the site of your laboratory in Ajaccio, Corsica.

We successively varied the fluid flow rate, the air thickness between cover and absorber (reduction of convective losses by the front face), the insulation thickness (decrease of back and lateral thermal losses) and the cover emissivity (decrease of front radiative losses).

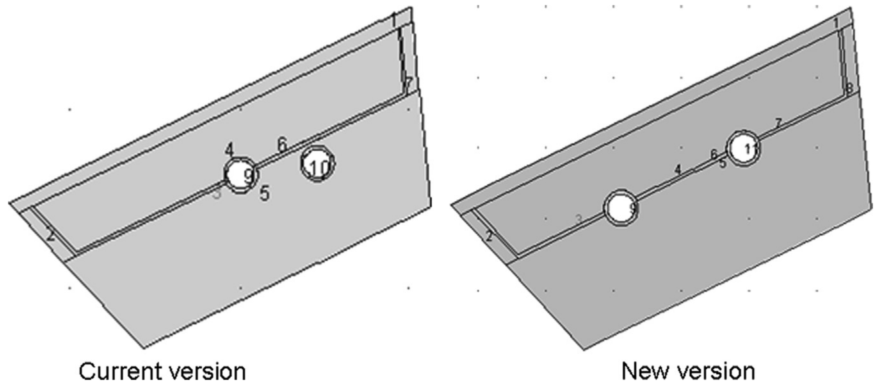


Fig. 12. The two versions of the solar collector H2OSS used for the optimization.

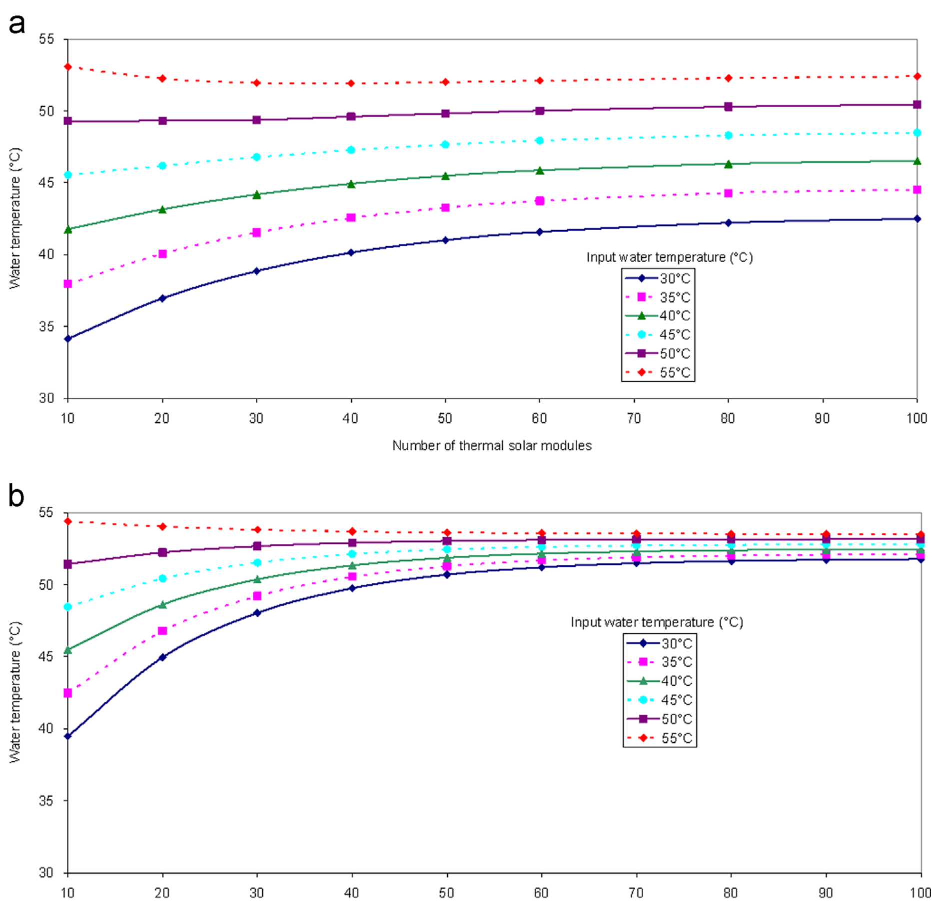


Fig. 13. Evolution of the water temperature versus the number of solar thermal modules for (a) the current version and (b) the new version of solar collector.

The domain of variation of these parameters must be realistic for two reasons: the dimensions of the solar collector must stay in the commercial standards and the gutter must continue to evacuate the rainwater (limits of the thermal insulation). In view to illustrate the calculations realized for each configuration of the solar collector, we show in Table 2, the various monthly energies (January and July) previously presented for the "current" configuration.

We note that the monthly energy needs in winter and summer are slightly different (2%) because in summer the mean temperature of the storage tank is slightly higher than in winter.

We also note that the values of the three solar fractions are very different particularly during summer because the running time of the electrical pump is greater in this period of the year. We can therefore expect different results in the optimization phase according to the chosen solar fraction.

4.2. Influence of the flow rate

Using a low flow rate allows a thermal stratification of the storage, a reduction of the hydraulic losses and consequently a small pump power and tube diameter [46,47]. Hollands and Lightstone [61] calculated an annual energy gain of 38% compared with a solar system with high flow rate and Cristofari et al. [45] an annual gain of 5.25%. As we saw previously, the hydraulic losses are high and then, using FR^{+} and FR^{++} (taking into account the electrical consumption of the pump) should modify the optimization results compared with the use of FR.

We see in Fig. 14 (and Fig. 13) that the performances of the new version of the solar collector are higher than for the current version. Thus, in the following optimization, we will only consider the new version.

The optimal flow rate is more visible using SF^{+} and SF^{++} than SF; furthermore SF^{+} and SF^{++} are more representative of the performance level of the thermal system because the significant electrical consumption of the water pump is taken into account. The optimal flow rates are respectively 50 L h^{-1} and 75 L h^{-1} for summer and winter for the new configuration, and around 75 L h^{-1} for the current one. For the winter period, the performances gap between the two rates, 50 L h^{-1} and 75 L h^{-1}, is lower

Table 2
Example of calculation of the solar fractions for the current configuration of the solar collector in January and July.

		January	July
Thermal energy drawn to the storage tank	kWh	182.3	171.7
Thermal losses (storage tank and water distribution circuit)	kWh	27.8	43.9
Thermal energy needs	kWh	210.1	215.6
Thermal energy produced by the solar resource	kWh	51.1	146.6
Running time of the pump	h	62.5	219
Electrical energy for the pump	kWh	6.2	21.9
Running time of the auxiliary electric heater	h	79	34.5
Electrical consumption of the auxiliary heater	kWh	159	69
Solar Fraction, SF	%	24.3	68
Solar Fraction, SF^{+}	%	23.6	61.7
Solar Fraction, SF^{++}	%	18.6	38.0

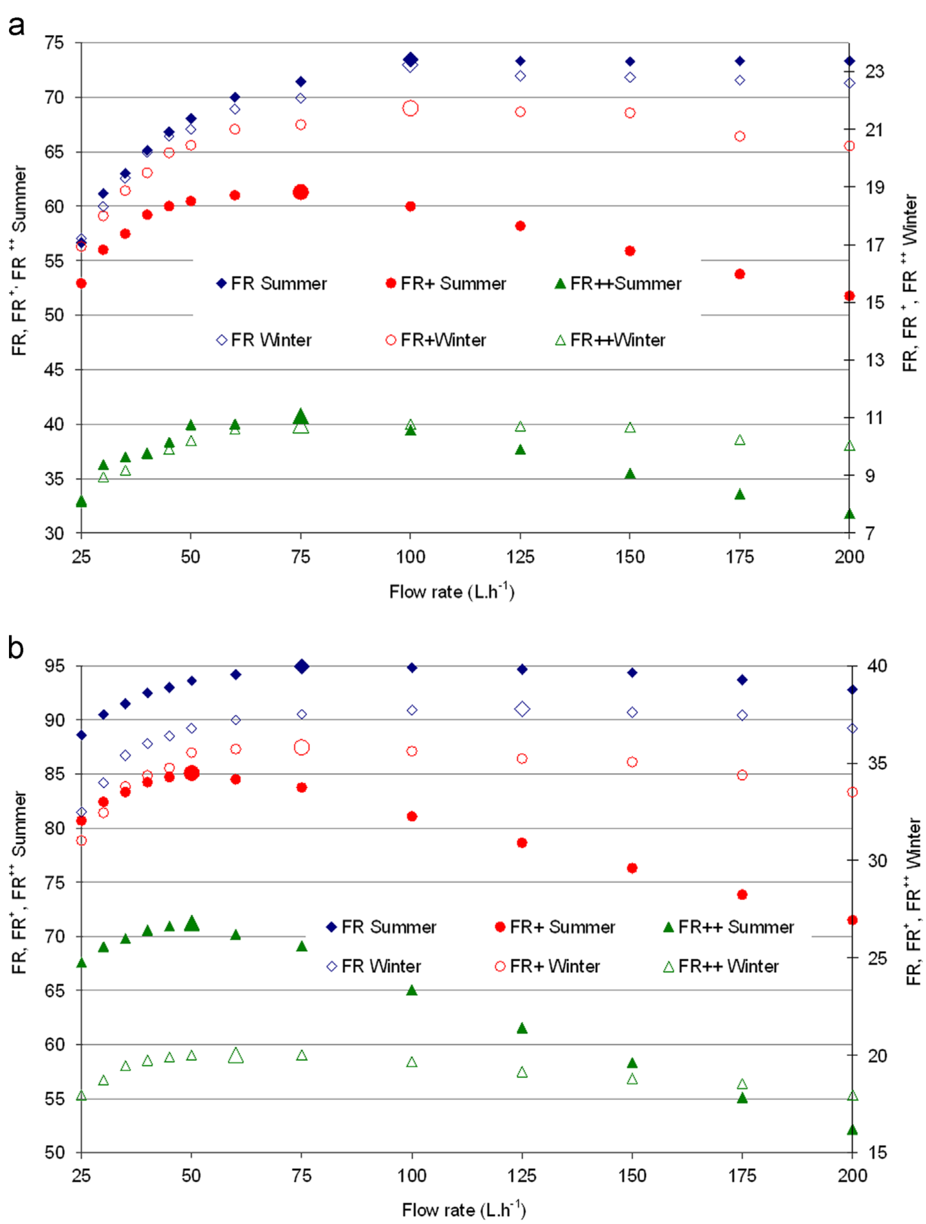


Fig. 14. The various solar fractions versus the water flow rate for (a) the current version and (b) the new version of the solar collector.

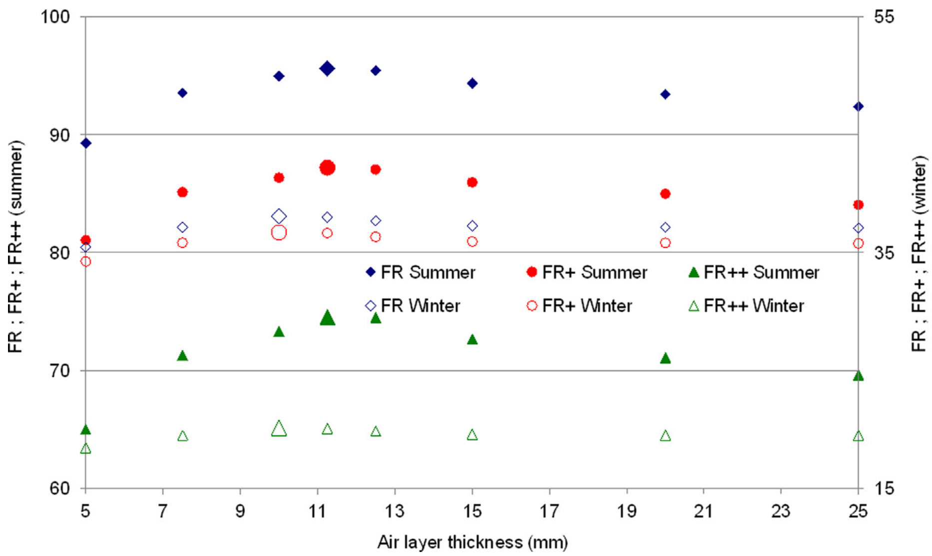


Fig. 15. SF, SF^{+} and SF^{++} versus the air layer thickness.

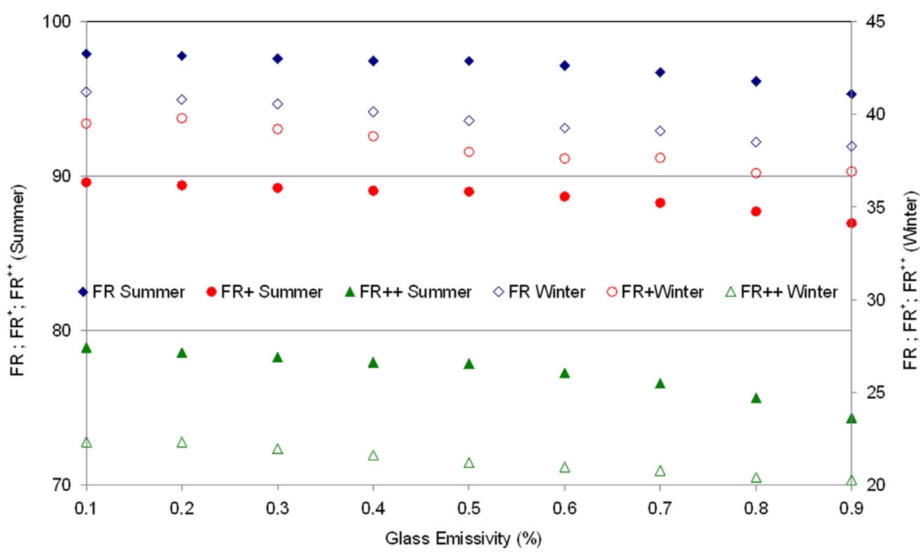


Fig. 16. Influence of the cover emissivity on the solar fractions.

than in the summer period, thus, the optimum water flow rate for the new version is taken at 50 L h^{-1}. Thus, the optimization calculations will be realized for 50 L h^{-1}; which is a low flow rate because is considered as a low flow rate, a value between 7 and 15 L h^{-1} m^{-2} [62] i.e. for our 4 m² between 28 and 60 L h^{-1}.

4.3. Optimisation of the air thickness

Various authors studied the optimal thickness for the air layer between the glass cover and the absorber: Holland et al. [63] and Baum and Ovezsakhatov [64] wrote that a thickness from 1 to 2 cm is adequate; Duffie and Beckman [43] and more recently Ferahta et al. [65] confirmed that 1 cm is the optimal thickness.

We calculated the three solar fractions for various air thicknesses (Fig. 15).

The form of the curve is due to the variation of the convective coefficient into the air layer as shown by Nahar and Garg [66]. As previously, it appears two optimums: 1 cm for winter and 1.125 cm for summer. We note that the optimum value of the air thickness is the same whatever the solar fraction is because the influence of the pump electrical consumption is very small and approximately always the same (the flow rate being constant). We chose an optimal value of 1.125 cm of air thickness what is in good accordance with the literature.

4.4. Optimisation of the cover emissivity

The glass emissivity influences the thermal production: lower is the emissivity, better is the performances. A glass with a low emissivity being more expensive that a conventional one, it is interesting to know if the gain can justify an increase of the glass cost. In the present version, the solar collector uses a convention glass with an emissivity equal to 0.9 but it exists on the market with affordable prices, some specific glasses with an emissivity reaching 0.1 in with the disposition of a thin film on the glass reducing the transmittance from 0.89 to 0.81 [67]. In our simulation this transmittance reduction has been taken into account and the results are shown in Fig. 16.

The gain on the solar fraction SF is between 2.6% and 3% i.e. in relative value between 3% and 8%. It seems interesting to use this type of cover.

4.5. *Optimisation of the thermal insulation thickness in the backside*

In view to characterize the influence of the thermal insulation in the back face, we realized several simulations in varying the height of the 3 isothermal elements l1, l2 and l3 in stone wool (Fig. 17). It seems obvious that the influence will be smaller for the two layers farthest from the absorber (i.e. l2 and l3).

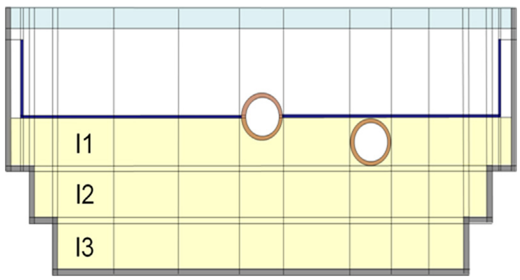


Fig. 17. The various thermal insulation layers.

The simulations show that an increase of the heights of the elements l2 and l3 does not influence the performances. For the element l1, the results are shown in Fig. 18.

The maximal improvement is very low: not more than 1% in absolute value on SF. This increase of the thermal insulation has a small influence which confirms the predominance of the edge effects in the thermal behaviour of this solar collector. The thermal insulation thickness will be not modified because the influence is low, moreover a good rainwater evacuation must be preserved.

4.6. *Optimisation of the thermal insulation between the absorber and the aluminium body*

The absorbers fins, very hot elements, are insulated from the aluminium body (very diffusive material) by only 2 mm of Makrolon® (polycarbonate product) (see Fig. 2). In our simulation we added insulation between the fins and the body without decreasing the collecting surface; we tested various thicknesses up to 16 mm for each side, but the maximum usable thickness is 4 mm for a standard gutter with a good rainwater evacuation (Fig. 19).

We see that from a thickness of 4–5 mm, the curves tend towards an asymptote. With a Makrolon® insulation of 4 mm on

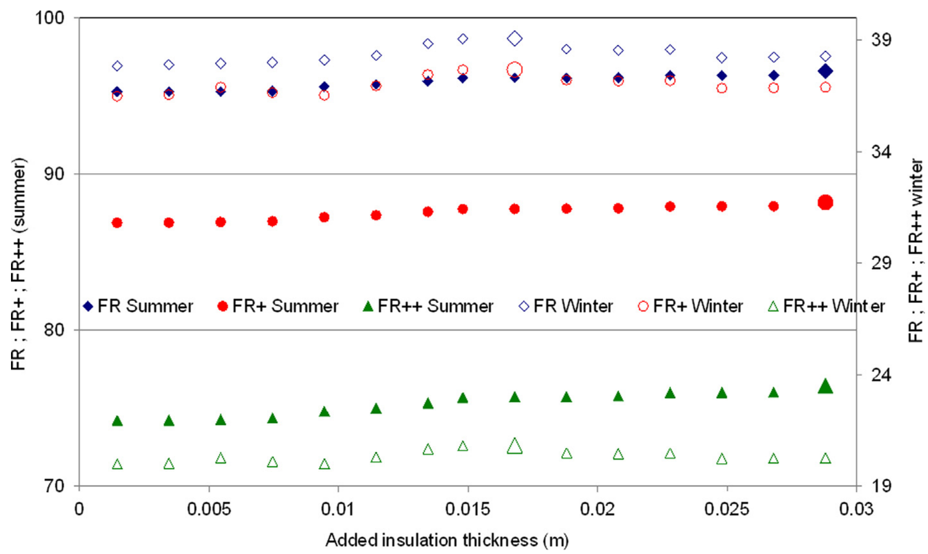


Fig. 18. Influence of the thermal insulation thickness of the layer l1.

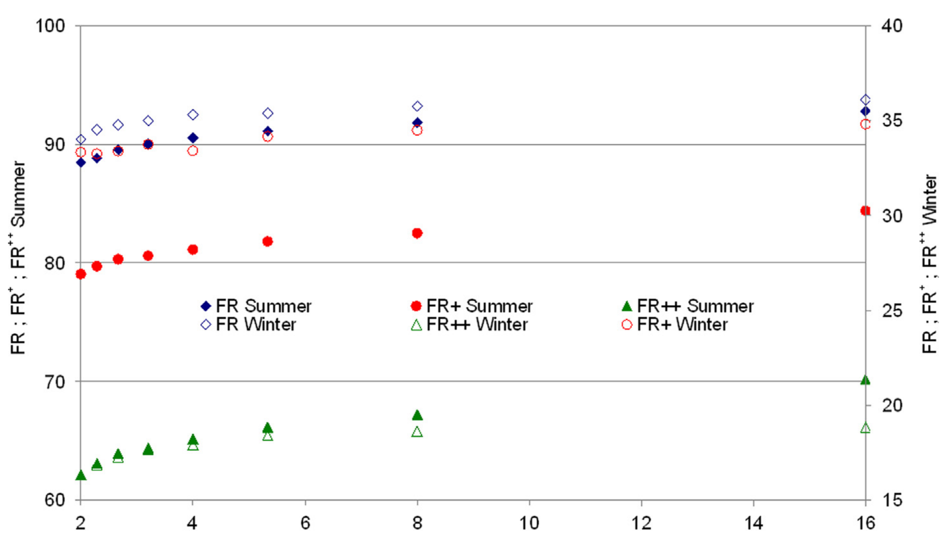


Fig. 19. Influence of the Makrolon® thickness between the absorber fins and the aluminium body.

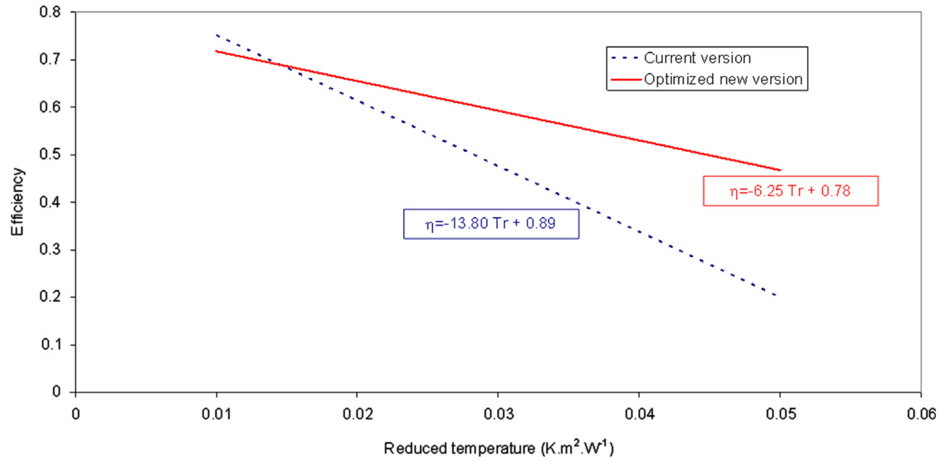


Fig. 20. Performances straight lines for current and optimized new versions (calculated from simulation).

Table 3
Synthesis of the main optimization results.

Parameter	Optimal value
Water tubes position	Into the absorber (the cold tube is no longer in the insulation)
Flow rate	50 L h^{-1}
Air layer thickness	1.125 cm
Glass cover emissivity	0.1
Backside thermal insulation	No more
Makrolon® insulation	+2 mm in both sides

both sides (2 mm more that in the present version) we obtain an improvement of 1.3% in winter (+4%) and 2% in summer (+2.26%) for SF.

4.7. Recap of the optimization

From previous results, we created an ⟨ideal⟩ H2OSS® solar collector with characteristics that are summarized in Table 3 for a solar installation for 4 persons, situated in the South of France with the daily water load profile seen in Fig. 9. and constituted by 35 m of solar modules (4 m²) and a water storage of 200 L.

In view to see clearly the consequences of this optimization on the thermal performances of the solar thermal system, we plotted in Fig. 20 the efficiency versus the reduced temperature for the current solar collector and the new optimized version. These two straight lines are calculated from a numerical simulation. In Fig. 4 the straight line for the current version in serial configuration was determined experimentally and we compare it with Fig. 20, we note a very good concordance between the experimental and numerical results which confirms the accuracy of the numerical model.

If we compare the current version and the new one, we note that the thermal losses coefficient decreases from 13.80 W m^{-2} K^{-1} to 6.25 W m^{-2} K^{-1} (i.e. an improvement of more than 50%) but the optical coefficient decreases from 0.903 to 0.780 (−13%) due to the replacement of the glass cover by a low emissivity one inducing a smaller transmittance.

Despite the improvement of the thermal losses coefficient, it stays higher than that of the Buderus 3.0. (4.3 W m^{-2} K^{-1}).

5. Conclusion

The numerical models developed in this work allowed to propose new configurations for the H2OSS thermal solar collector on the basis of experimental findings. The solar collector was optimized numerically for a conventional installation for an individual housing in the South of France. The new positioning of the cold water tube into the absorber, and no more in the insulation, allows to reach much better performances than with the actual prototype (the annual fraction passes from 41% for the current version to 76% for the optimized version). The thermal insulation and the air layer thickness have been optimized; the influence of the water flow rate was very important due to the particular linear conception of the H2OSS collector and the optimization showed the necessity to work at low flow rate.

This new configuration of the H2OSS concept will be implemented soon in the form of a prototype and it will be able to validate experimentally the numerical results.

Acknowledgement

The authors thank the Territorial Collectivity of Corsica and OSEO-ANVAR for their financial supports. This work was realized in the framework of the COST Action TU1205 on “Building Integration of Solar Thermal Systems (BISTS)”.

References

[1] Reisinger H, Dulle, Henao, Pittermann. Monograph: house of the future. Annex 7. VLEEM – very long term energy environment modelling. EC/DG research contract ENG2-CT-2000-00441, Final report; August 2002 ⟨vleem.org⟩.
[2] Munari Probst MC, Roecker C. Towards an improved architectural quality of building integrated solar thermal systems (BIST). Sol Energy 2007;81:1104–16.
[3] D'Antoni M, Saro O. Massive, solar–thermal collectors: a critical literature review. Renew Sustain Energy Rev 2012;16(6):3666–79.
[4] Affolter P, Eisenmann W, Fechner H, Rommel M, Schaap A, Serensen H., et al. PVT roadmap: a European guide for the development and market introduction of PV–thermal technology. ECN Editor; 2007.
[5] Delisle V, Kummert M. A novel approach to compare building-integrated photovoltaics/thermal air collectors to side-by-side PV modules and solar thermal collectors. Sol Energy 2014;100:50–65.
[6] Chow TT. A review on photovoltaic/thermal hybrid solar technologies. Appl Energy 2010;87(2):365–79.

[7] Ibrahim A, Othman MY, Ruslan MH, Mat Sohif, Sopian Kamaruzzaman. Recent advances in flat plate photovoltaic/thermal (PV/T) solar collectors. Renew Sustain Energy Rev 2011;15(1):352–65.
[8] Tyagi VV, Kaushik SC, Tyagi SK. Advancement in solar photovoltaic/thermal (PV/T) hybrid collector technology. Renew Sustain Energy Rev 2012;16 (3):1383–98.
[9] Kumar R, Rosen MA. A critical review of photovoltaic-thermal solar collectors for air heating. Appl Energy 2011;88(11):3603–14.
[10] Hussain F, Othman MYH, Sopian K, Yatim B, Ruslan H, Othman H. Design development and performance evaluation of photovoltaic/thermal (PV/T) air base solar collector. Renew Sustain Energy Rev 2013;25:431–41.
[11] Vats K, Tiwari GN. Energy and exergy analysis of a building integrated semitransparent photovoltaic thermal (BISPVT) system. Appl Energy 2012;96: 409–16.
[12] Gaur MK, Tiwari GN. Optimization of number of collectors for integrated PV/T hybrid active solar still. Appl Energy 2010;87(5):1763–72.
[13] Bakker M, Zondag HA, Elswijk MJ, Strootman KJ, Jong MJM. Performance and costs of a roof-sized PV/thermal array combined with a ground coupled heat pump. Sol Energy 2005;78:331–9.
[14] Zogou O, Stapountzis H. Energy analysis of an improved concept of integrated PV panels in an office building in central Greece. Appl Energy 2011;88 (3):853–66.
[15] De Beijer. Product development in solar water heating. Renew Energy 1998;15:201–4.
[16] Robin JM. Fixed or mobile device of closure for openings in buildings, capable of capturing solar energy. European Patent no. EP1376026. 27.06.2003. Available at: 〈https://register.epo.org〉.
[17] Chen K, Oh SJ, Kim NJ, Lee YJ, Chun WG. Fabrication and testing of a non-glass vacuum-tube collector for solar energy utilization. Energy 2010;35 (6):2674–80.
[18] Rassamakin B, Khairnasov S, Zaripov V, Rassamakin A, Alforova O. Aluminum heat pipes applied in solar collectors. Sol Energy 2013;94:145–54.
[19] Glembin J, Rockendorf G, Scheuren J. Internal thermal coupling in direct-flow coaxial vacuum tube collectors. Sol Energy 2010;84(7):1137–46.
[20] Fernández A, Dieste JA. Low and medium temperature solar thermal collector based in innovative materials and improved heat exchange performance. Energy Convers Manag 2013;75:118–29.
[21] Kalogirou SA. Low concentration ratio solar collectors. Reference module in earth systems and environmental sciences. Compr Renew Energy 2012;3: 149–63.
[22] Nkwetta DN, Smyth M, Zacharopoulos A, Hyde T. In-door experimental analysis of concentrated and non-concentrated evacuated tube heat pipe collectors for medium temperature applications. Energy Build 2012;47: 674–81.
[23] Shah LJ, Furbo S. Vertical evacuated tubular-collectors utilizing solar radiation from all directions. Appl Energy 2004;78(4):371–95.
[24] Tiago M, Oliveira Armando C. Energy and economic analysis of an integrated solar absorption cooling and heating system in different building types and climates. Appl Energy 2009;86:949–57.
[25] Nkwetta DN, Smyth M. Performance analysis and comparison of concentrated evacuated tube heat pipes solar collectors. Appl Energy 2012;98:22–32.
[26] Karami M, Akhavan Bahabadi MA, Delfani S, Ghozatloo A. A new application of carbon nanotubes nanofluid as working fluid of low-temperature direct absorption solar collector. Sol Energy Mater Sol Cells 2014;121:114–8.
[27] Rana P, Bhargava R. Flow and heat transfer of a nanofluid over a nonlinearly stretching sheet: a numerical study. Commun Nonlinear Sci Numer Simul 2012;17:212–26.
[28] Rana P, Bhargava R. Mixed convective heat transfer flow of nanofluid past a permeable vertical flat plate with magnetic effects: a Finite Element study. Appl Mech Mater 2012;110–116:3679–87.
[29] Javadi FS, Saidur R, Kamalisarvestani M. Investigating performance improvement of solar collectors by using nanofluids. Renew Sustain Energy Rev 2013;28:232–45.
[30] Tyagi H, Phelan P, Prasher R. Predicted efficiency of a low-temperature nanofluid-based direct absorption solar collector. J Sol Energy Eng, Trans ASME 2009;131(4):0410041–7.
[31] Yousefi T, Veizy F, Shojaeizadeh E, Zinadini S. An experimental investigation on the effect of MWCNT-H_2O nanofluid on the efficiency of flat-plate solar collectors. Exp Therm Fluid Sci 2012;39:207–12.
[32] Colangelo G, Favale E, De Risi A, Laforgia D. Results of experimental investigations on the heat conductivity of nanofluids based on diathermic oil for high temperature applications. Appl Energy 2012;97:828–33.
[33] Colangelo G, Favale E, De Risi A, Laforgia D. A new solution for reduced sedimentation flat panel solar thermal collector using nanofluids. Appl Energy 2013;111:80–93.
[34] Faizal M, Saidur R, Mekhilef S. Potential of size reduction of flat-plate solar collectors when applying MWCNT nanofluid. In: Proceedings of the 4th international conference on energy and environment, IOP conference series: earth and environmental science, vol. 16; 2013.
[35] Hassan MM, Beliveau Y. Design, construction and performance prediction of integrated solar roof collectors using finite element analysis. Constr Build Mater 2007;21:1069–78.
[36] De Beijer. Product development in solar water heating. Renew Energy 1998;15:201–4.
[37] Huang BJ Lin YH, Ton WZ, Hou TF, Chuang YH. Building-integrated solar collector (BISC). In: Proceedings of the world renewable energy congress. Linköping, Sweden; 8–13 May 2011. p. 3718–25.
[38] Canaletti JL, Notton G, Cristofari C. New concept of solar air heater integrated in the building. ISJAEE 2008;5:39–44.
[39] Cristofari C. Device for collecting rainwater and solar energy originating from light radiation. Patent no. WO 2006/100395 A1; 28.09.2006.
[40] Motte F, Notton G, Cristofari C, Canaletti JL. Design and modelling of a new patented thermal solar collector with high building integration. Appl Energy 2013;102:631–9.
[41] Haillot D, Nepveu F, Goetz V, Py X, Benabdelkarim M. High performance storage composite for the enhancement of solar domestic hot water systems Part 2: numerical system analysis. Sol Energy 2012;1:64–77.
[42] European Standard EN 12975-1. Thermal solar systems and components – solar collectors – Part 1: general requirements. March 2006.
[43] Duffie JA, Beckman WA. Solar engineering on thermal process. New York: John Wiley & Sons Ed.; 2006.
[44] Incropera FP, DeWitt DP, Bergman TL, Lavine AS. Fundamentals of heat and mass transfer. 6th ed.. USA: John Wiley; 2007.
[45] Cristofari C, Notton G, Poggi P, Louche A. Influence of the flow rate and the tank stratification degree on the performances of a solar flat-plate collector. Int J Therm Sci 2003;42(5):455–69.
[46] Shah LJ. Investigation and modeling of thermal conditions in low flow SDHW systems. Department of Buildings and Energy Technical University of Denmark Report R-034; 1999.
[47] Furbo S. Optimum design of small DHW low flow solar heating systems. ISES Solar World Congress Budapest Report 93-24; 1993.
[48] Haillot D. Matériaux composites à hautes performances énergétiques pour l'optimisation des chauffe-eau solaires individuels: du matériau au procédé (Ph.D. dissertation). University of Perpignan, France; 2009.
[49] Mather D, Hollands KG, Wright J. Single- and multi-tank energy storage for solar heating systems: fundamentals. Sol Energy 2002;73:3–13.
[50] Nepveu F. Production décentralisée d'électricité et de chaleur par système Parabole/Stirling: application au système EURODISH (Ph.D. dissertation). University of Perpignan; 2008.
[51] Shah K, Mueller AC. Heat exchangers. In: Rohsenow WM, Hartnett JP, Ganic EN, editors. Handbook of heat transfer applications. New York: Mc Graw Hill; 1985.
[52] NF EN 13203-1. Appareils domestiques produisant de l'eau chaude sanitaire utilisant les combustibles gazeux, Appareils de débit calorifique inferieur ou égal à 70 kW et de capacité de stockage inférieure ou égale à 300 l, Partie 1: evaluation de la performance en puisage d'eau chaude. European standard; 2006.
[53] Buscarlet C, Caccavelli D. Suivi et évaluation énergétique du Plan Soleil: Chauffe-eau solaires individuels. CSTB report, DD/ENR-035 RS; July 2006 〈enr.cstb.fr〉.
[54] ADEME. Réduction des consommations d'énergie pour l'ECS. Technical Sheet; 03.01.2006.
[55] Wagner & Co. Système de montage sur toiture TRICA pour capteur EURO; 2011 〈www.wagner-solar.com〉.
[56] Buderus SKN. 3.0 Installation manual – flate plate collectors; 2007.
[57] Huang BJ, Lin TH, Hung WC, Sun FS. Performance evaluation of solar photovoltaic/thermal systems. Sol Energy 2001;70:443–8.
[58] Tiwari A, Sodha MS. Performance evaluation of hybrid PV/thermal water/air heating system: a parametric study. Renew Energy 2006;31:2460–74.
[59] Tiwari A, Sodha MS. Performance evaluation of hybrid PV/thermal water/air heating system: an experimental validation. Sol Energy 2006;80:751–9.
[60] Tiwari A, Sodha MS. Parametric study of various configurations of hybrid PV/thermal air collector: experimental validation of theoretical model. Sol Energy Mater Sol Cells 2007;91:17–28.
[61] K.G.T. Hollands, Lightstone MF. A review of low flow, stratified-tank solar water heating systems. Sol Energy 1989;43(2):97–105.
[62] Kenjo L, Inard C, Caccavelli D. Experimental and numerical study of thermal stratification in a mantle tank of a solar domestic hot water system. Appl Therm Eng 2007;27(11–12):1986–95.
[63] K.G.T. Hollands, Raithby GD, Unny TE. Methods for reducing heat losses from flat plate solar collectors, phase 2. Final report. Ontario: Waterloo University; 1978 (1 February 1976–31 August 1977).
[64] Baum VA, Ovezsakhatov N. Convectives losses through an air filled gap. Geliotekhnika 1976;120:33–5.
[65] Ferahta FZ, Bougoul S, Ababsa D, Abid C. Numerical study of the convection in the air gap of a solar collector. Energy Proc 2011;6:177–85.
[66] Nahar NM, Garg HP. Free convection and shading due to gap spacing between an absorber plate and the cover glazing in solar energy flat-plate collectors. Appl Energy 1980;7(1–3):129–45.
[67] AGC Glass; 2013, web site: 〈www.yourglass.com/〉.